E-21-6TQ
N/A

MNA-SP

Numerical Convolution-based tool
to analyze transmission lines characterized
by bandlimited S-parameters and terminated
by passive circuits

Georgia Tech College of Engineering

Prof. Madhavan Swaminathan
School of Electrical and Computer Engineering
Georgia Institute of Technology
Atlanta, GA 30332.
madhavan.swaminathan@ece.gatech.edu

Causal Transient Simulation of Systems Characterized by Frequency-Domain Data in a Modified Nodal Analysis Framework

S. N. Lalgudi[1], K. Srinivasan[1], G. Casinovi[1], R. Mandrekar[1], E. Engin[1], M. Swaminathan[1], and Y. Kretchmer[2]

[1]Georgia Institute of Technology, Electrical and Computer Engg. department, Atlanta, GA, USA.
gtg228q@mail.gatech.edu,{krishna, giorgio.casinovi, rohan, engin, madhavan.swaminathan}@ece.gatech.edu

[2]Altera Corporation, San Jose, CA, USA.
ykretchm@altera.com

Abstract

In this paper, an approach for the causal transient simulation of the sampled frequency-domain data in a modified nodal analysis (MNA) framework has been proposed. The causality of the transient results has been explicitly enforced from the port-to-port propagation delay, which has been extracted from the frequency data. Results demonstrating the accuracy of the proposed approach have been presented.

I. Introduction

Transient simulation using frequency-domain parameters is an accurate and memory- and time-efficient approach for modeling interconnects with frequency-dependent electrical properties [1]- [3]. In some applications, a part of the geometry is characterized by frequency-domain parameters and the rest is characterized by a SPICE-like circuit. For instance, while cosimulating power-supply noise in the power distribution networks (PDN) of the chip and the package, the on-chip PDN is usually characterized by a distributed equivalent circuit, and the package PDN is usually characterized by a frequency-domain data. In such instances, the transient simulation engine should integrate the frequency-domain data with the rest of the SPICE circuitry. Also, since the geometry characterized by the frequency-domain data can be electrically long, the propagation delay of a signal through the geometry cannot be ignored. In some cases, when the propagation delay is not correctly captured, the switching noise can be estimated inaccurately [2]. Therefore, developing a causal transient simulation engine that can take in both the frequency-domain data and the SPICE-like circuit is important.

A transient simulation approach that takes in band-limited scattering parameters (S-parameters) for analyzing lossy transmission lines terminated with linear/nonlinear sources/loads has been proposed in [1]. To enable time-domain simulation, the scattering parameters are converted to time domain using the inverse discrete fourier transform (IDFT). At each time step of transient simulation, the port voltages and currents are obtained through a numerical convolution. In [2], the technique proposed in [1] has been used to simulate power-supply noise in the package signal and power distribution networks (PDN) characterized by band-limited S-parameter data. Since the power planes and the signal lines in the package are electrically long, the propagation delay through them cannot be ignored. In [2], a technique that correctly captures the propagation delay between the ports has been presented. This technique enforces causality (i.e., models propagation delay) of the transient results only with the knowledge of the S-parameters and without any knowledge of the geometry that is being characterized by these S-parameters. However, the formulation presented in [2] requires computing reflection and transmission coefficients looking out of each port. These coefficients can be easily computed when the ports are terminated with simple circuits such as a complex linear load or a nonlinear source. However, if the ports are connected to a complicated SPICE-like circuit, then the reflection and transmission coefficients cannot be easily computed. Therefore, in such instances, the formulation in [2] cannot be applied and has to be extended.

In this paper, the formulation presented in [2] has been extended to cosimulate the S-parameter data of a subnetwork with the SPICE-like netlist of the rest of the network. The new formulation integrates the formulation in [1], [2] for the subnetworks that are characterized by frequency-domain data with the modified nodal analysis (MNA) formulation [4] of the rest of the network. Since the rest of the network including the port terminations are accounted for in the MNA formulation, there is no need to compute the reflection and transmission coefficients looking out of each port. The new formulation is more general than the formulation in [2] and can be used to simulate subnetworks that are characterized by frequency-domain data with the rest of the network that is characterized by a SPICE-like netlist.

The authors of [1] have also integrated their formulation in a MNA framework in [3]. However, unlike in [1], the S-parameters are modeled by reduced-order rational functions. As a result, the convolution can be computed semi-analytically and recursively. Recursive convolution helps in reducing the time complexity of convolution from super-linear to linear run

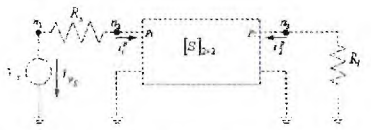

Fig. 1. Two-port S-parameter network terminated with a voltage source at port 1 and a resistor at port 2.

time in the number of time steps. However, in a rational-function based approach, computing the coefficients of the numerator and denominator polynomials of the rational function requires solving ill-conditioned matrices, which can compromise the accuracy of the transient simulation. Also, the maximum number of ports that can be simulated using rational function-based approaches are usually very small ($\leq$ 40 ports). On the other hand, the new formulation proposed in this paper does not fit any rational functions, and hence, is not plagued by inaccuracy issues associated with the rational function-based approaches. Also, the number of ports that can be simulated is large ($>$ 100 ports, see [2]).

The rest of the paper is organized is as follows. In Section II, the formulation integrating the frequency-data in a MNA framework is described. In Section III, the technique for enforcing causality is explained. In Section IV, the results demonstrating the accuracy of the proposed approach are shown. Finally, in Section V, the conclusions of this paper are reported.

II. Formulation

In this section, the formulation for integrating the frequency-domain data in the MNA framework is described. For simplicity, the formulation is described for a 2-port example shown in Figure 1. In Figure 1, n_i denotes node i, p_i denotes port i, R_s denotes the source resistance, R_l denotes the load resistance, $v_s(t)$ denotes the time-varying voltage source, $[S]_{N_p \times N_p}$ denotes the band-limited S-parameters characterizing the subnetwork with N_p ports, $i_{v_s}(t)$ denotes the current through voltage source at time t, and $i_j^p(t)$ denotes the current entering p_j at time t. Let $a_i(t)$ and $b_i(t)$ denote the voltage waves entering and leaving port i at time t , respectively. Let Δt be the time step, ω be the angular frequency, $\overline{x}(t) = \begin{bmatrix} x_1(t) & x_2(t) \end{bmatrix}'$, $\overline{X}(\omega)$ denote the continuous fourier transform of $\overline{x}(t)$, $\overline{x}[n] = \overline{x}(n\Delta t)$, $\overline{\overline{X}}$ denote a matrix and X_{ij} denote the element corresponding to row i and column j in $\overline{\overline{X}}$. If Z_0 is the characteristic reference impedance, $Y_0 = 1/Z_0$, v_i is the voltage at node i, and v^{p_i} is the voltage at port i, then

$$\overline{i^p}(t) = Y_0 \left(\overline{a}(t) - \overline{b}(t) \right), \tag{1}$$

and

$$\overline{v^p}(t) = \overline{a}(t) + \overline{b}(t). \tag{2}$$

Let the symbol '$*$' denote linear convolution, and let '$*$' be defined numerically as

$$x(t) * g(t) = \sum_{m=1}^{n} x[n-m]g[m]\Delta t. \tag{3}$$

When the relation $\overline{B}(\omega) = \overline{\overline{S}}(\omega)\overline{A}(\omega)$ is converted to time domain through inverse fourier transform (IFT), which is computed numerically from IDFT, $\overline{a}$ and $\overline{b}$ can related through convolution:

$$\overline{b}(t) = \overline{\overline{s}}(t) * \overline{a}(t). \tag{4}$$

When the definition in (3) is employed in (4), $\overline{a}[n]$ and $\overline{b}[n]$ can be related as

$$\overline{\overline{s}}[0]\Delta t\overline{a}[n] + \overline{b}[n] = \overline{h}[n], \tag{5}$$

where

$$h_i[n] = \sum_{m=1}^{n-1} \sum_{j=1}^{N_p} s_{ij}[n-m]a_j[m]\Delta t. \tag{6}$$

The time complexity of computing h_i directly from (6) for all N_t time steps is $\mathcal{O}(N_p N_t^2)$. However, this complexity can be reduced to $\mathcal{O}(N_p N_t \log(N_p))$ using fast convolution methods, as described in [2].

The port voltages $\overline{v^p}$ and $\overline{i^p}$ can be related through (5) using (1) and (2). To relate $\overline{v^p}$ and $\overline{i^p}$ to v_s, MNA of the rest of the network is performed. MNA requires solving the Kirchoff's current laws (KCL) of all the nodes with the Kirchoff's voltage laws for all the voltage sources and the inductors. The KCLs at n_1, n_2, and n_3 and the KVL for v_s are given, respectively, by

$$\begin{aligned} \tfrac{v_1(t)-v_2(t)}{R_s} + i_{v_s}(t) &= 0, \\ \tfrac{v_2(t)-v_1(t)}{R_s} + i_1^p(t) &= 0, \\ \tfrac{v_3(t)}{R_l} + i_2^p(t) &= 0, \text{ and} \\ v_1(t) &= v_s(t). \end{aligned} \tag{7}$$

Since the KCL at nodes that correspond to the ports depends on $\overline{i^p}$, which is still a unknown, (see the KCL at n_2 and n_3 in (7)), the KCs and the KVLs in the MNA should be solved along with (1), (2), and (5). This solution is possible at each time step as $v_s(t)$ and the term $h_i(t)$ are known at the time. From the solution, the voltages at all nodes, including the voltage at the ports, can be computed at each time step. If the number of equations from MNA is M (in the example above, $M = 4$), then size of the system to be solved is is $(M + 2N_p)$.

III. Causality Enforcement

The transient result from the formulation described in Section II cannot strictly capture the port-to-port propagation delay if the impulse responses are computed from the actual band-limited S-parameters [2]. For a causal result, the port-to-port propagation delay has to be enforced explicitly in the transient solution. The extraction of the port-to-port propagation delay and the technique for enforcing this delay in the transient solution are described in detail in [2] and in brief below. The idea is based on the fact that for a causal signal, the real and imaginary parts of the signal in frequency domain are related through Hilbert transform relationship [5].

If T_{ij} is the propagation delay between ports p_i and p_j, then the transfer function $S_{ij}(\omega)$ of any generalized linear-phase system [5] between p_i and p_j can be decomposed as the product of its minimum-phase and all-pass components [5]:

$$S_{ij}(\omega) = S_{\min_{ij}}(\omega)e^{-l\omega T_{ij}}, \tag{8}$$

where $l = \sqrt{-1}$, $S_{\min_{ij}}(\omega)$ is the minimum-phase component of $S_{ij}(\omega)$, and $e^{-l\omega T_{ij}}$ is its all-pass component. In time domain, (8) can be expressed as

$$s_{ij}(t) = s_{\min_{ij}}(t - T_{ij}). \tag{9}$$

If the decomposition in (8) is available, then causality can be enforced in the transient solution by using $\overline{\overline{s_{\min}}}(t)$ instead of $\overline{s}(t)$ in (4) - (??) and by zeropadding the transfer impulse response, $s_{\min_{ij}}(t)$, between p_i and p_j for $t \leq T_{ij}$. The decomposition in (8) can be obtained as follows. The magnitude of $S_{\min_{ij}}(\omega)$, $\left|S_{\min_{ij}}(\omega)\right|$, is obtained from (8) as

$$\left|S_{\min_{ij}}(\omega)\right| = \left|S_{ij}(\omega)\right|. \tag{10}$$

The phase of $S_{\min_{ij}}(\omega)$, $\arg\left(S_{\min_{ij}}(\omega)\right)$, can be computed from $\left|S_{\min_{ij}}(\omega)\right|$ through the Hilbert transform relationship [5]:

$$\arg\left(S_{\min_{ij}}(\omega)\right) = -\frac{1}{2\pi} P \int_{-\pi}^{\pi} \log\left(\left|S_{ij}(l\theta)\right|\right) \cot\left(\frac{\omega - \theta}{2}\right) d\theta, \tag{11}$$

where P is the Cauchy principal value. Therefore, $S_{\min_{ij}}(\omega)$ can be computed from (10) and (11) as

$$S_{\min_{ij}}(\omega) = \left|S_{\min_{ij}}(\omega)\right| e^{\arg(S_{\min_{ij}}(\omega))l}. \tag{12}$$

Knowing $S_{\min_{ij}}(\omega)$ from (12), T_{ij} can be computed from (8) as

$$T_{ij} = -\frac{1}{\omega} \arg\left(\frac{S_{ij}(\omega)}{S_{\min_{ij}}(\omega)}\right). \tag{13}$$

IV. Results

In this section, the accuracy of the proposed approach and the effect of not modeling causality correctly on signal integrity computations are demonstrated. The first test setup is as shown in Figure 2(a) in which the two-port subnetwork characterizes a transmission line, the voltage source is a one-volt step, $R_s = 0\ \Omega$, and $R_l = 25\ \Omega$. The S-parameters of the transmission line are obtained from 0-10 GHz using Agilent ADS. The step response at p_2 (see Figure 2(a)) is computed with and without enforcing causality. These two results are compared with the results from ADS and are shown in Figure 2(b-c). From Figure 2(b), it can be seen that the step response calculated without enforcing causality using the proposed approach matches well with the response calculated from ADS (the ADS results were obtained with the 0-10 GHz S-parameters data rather than with the transmission line model). This match demonstrates the accuracy of formulation that integrates the S-parameters in a MNA framework without enforcing causality. However, the step responses calculated both from the ADS and from the proposed approach without applying causality do not model the propagation delay: the step source is zero until 2.5 ns (see Figure 2(a)); the propagation delay through the line is 3 ns; therefore, the step response at p_2 should ideally be zero until 5.5 ns (= 2.5 ns + 3.5 ns); however, the responses from ADS and from proposed approach without enforcing causality appear at the far end of the line well before 5.5 ns (see Figure 2(b-c)). However, when the propagation delay is extracted and the causality is enforced following the description in Section III, the step response at p_2 is zero until 5.5 ns and follows a typical step response. This situation repeats every time (for example, at $t = 11.5$ ns and 17.5 ns in Figure 2(b)) a new reflected wave arrives at p_2, as can be seen in Figure 2(b). This result demonstrates both the accuracy of the proposed approach in capturing the port-to-port propagation delay and the accuracy of the overall formulation.

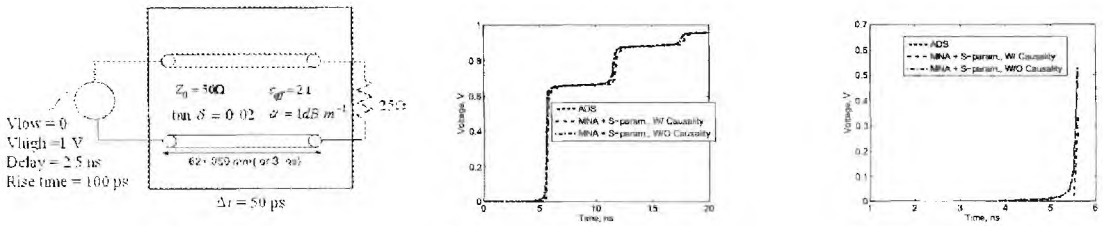

(a) Test setup. (b) Response from $t = 0 - 20$ ns. (c) Response from $t = 0 - 6$ ns.

Fig. 2. Comparison of the accuracy of causal transient simulation.

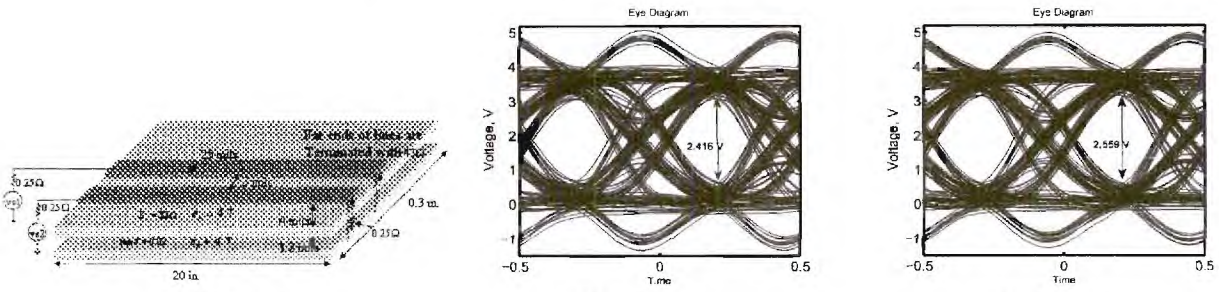

(a) Test setup. (b) w/o causality. (c) w/ causality.

Fig. 3. Comparison of effect of causality on the eye opening.

The second test setup consists of two coupled microstrip transmission lines referenced to a nonideal power-ground plane pair, as shown in Figure 3(a). The near ends of the lines are excited by a pseudo-random voltage source to simulate the output of a switching driver. The output voltage at the far end of one of the lines is computed using the formulation proposed in Section II. The two transmission lines and the power-ground plane pair are characterized by S-parameters between 0-2.5 GHz. The terminations are accounted for using the MNA. A bit in the pseudo-random sequence consists of a pulse with a rise time of 0.5 ns, a fall time of 0.5 ns, a peak time of 0.4 ns, and a period of 1.8e-9 ns. In this sequence, bit 0 represents 0 V and bit 1 represents 3.3 V. The eye pattern at the far end of the transmission lines and the eye opening are computed both with and without enforcing causality and are shown in Figure 3(b-c). From Figure 2(b-c), the eye opening without and with causality are observed to be 2.416 V and 2.559 V, respectively. Thus, without enforcing causality, there is an artificial closure of 142 mV. This result serves to demonstrate the effect of not enforcing causality strictly on signal integrity computations such as the eye diagram.

V. Conclusions

A causal transient simulation approach that integrates the frequency-domain data in a modified nodal analysis framework has been proposed. The transient results are made causal by extracting the port-to-port propagation delay from the frequency data and by enforcing this delay in the transient simulation. The accuracy of the proposed approach has been demonstrated. The proposed approach enables integrating the frequency-domain data of a subnetwork with any SPICE-like circuit of the rest of the circuitry. Since the proposed approach does not fit any rational functions to the transfer functions, the proposed approach would be accurate in the face of increasing number of ports and increasing bandwidth of the frequency data.

References

[1] J. E. Schutt-Aine, and R. Mittra, "Nonlinear transient analysis of coupled transmission lines," *IEEE Trans. on Circuits and Systems*, Vol. 36, No. 7, pp. 959–967, July 1989.

[2] R. Mandrekar, "Modeling and cosimulation of signal distribution and power delivery in packaged digital systems," Ph.D. Disseration, Dept. of Elect. Comput. Eng., Georgia Institute of Technology, Atlanta, 2006.

[3] W. T. Beyene, and J. E. Schutt-Aine, "Efficient transient simulation of high-speed interconnects characterized by sampled data," *IEEE Trans. on Components, Packaging, and Manufacturing Technology - Part B*, Vol. 21, No. 1, pp. 105–114, Feb. 1998.

[4] H. Chung-Wen, A. E. Ruehli, and P. A. Brennan, "The modified nodal analysis approach to network analysis," *IEEE Trans. on Circuits and Systems*, Vol. 22, No. 6, pp. 504–509, June 1975.

[5] A. Oppenheim, and R. Schafer, *"Discrete-time signal processing,"* 2nd edition, Prentice Hall, 1999, ch. 11.

Causal Transient Simulation of Systems Characterized by Frequency-Domain Data in a MNA Framework

Team: Subramanian N. Lalgudi, Krishna Srinivasan, Giorgio Casinovi,
Rohan Mandrekar*, Ege Engin, Madhavan Swaminathan, Yaron Kretchmer**

School of Electrical and Computer Engineering
Georgia Institute of Technology

***IBM, Austin, TX.**

****Altera Corporation, San Jose**

Objective

Causal transient simulation of frequency-domain data with SPICE circuits

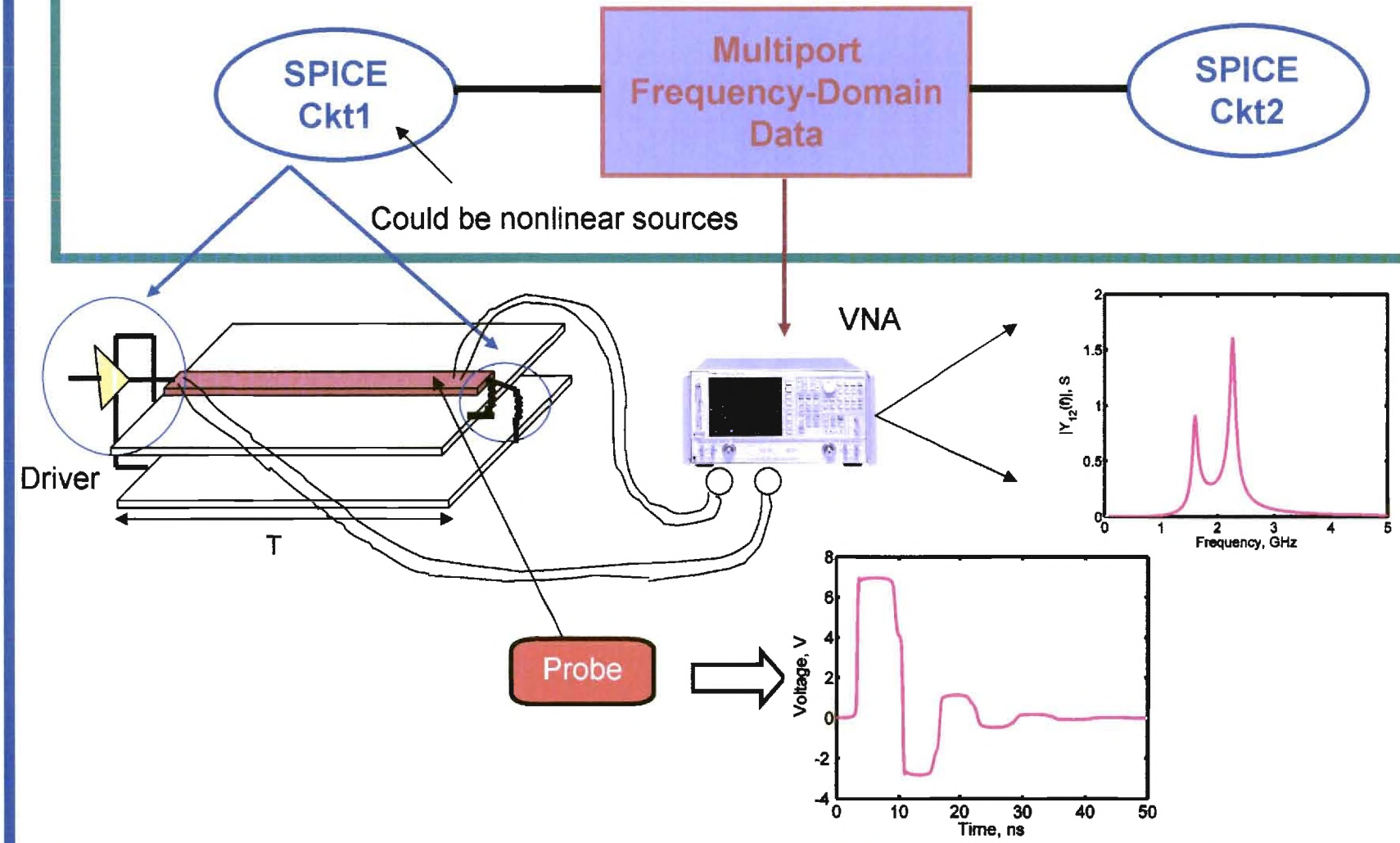

Need for Causality

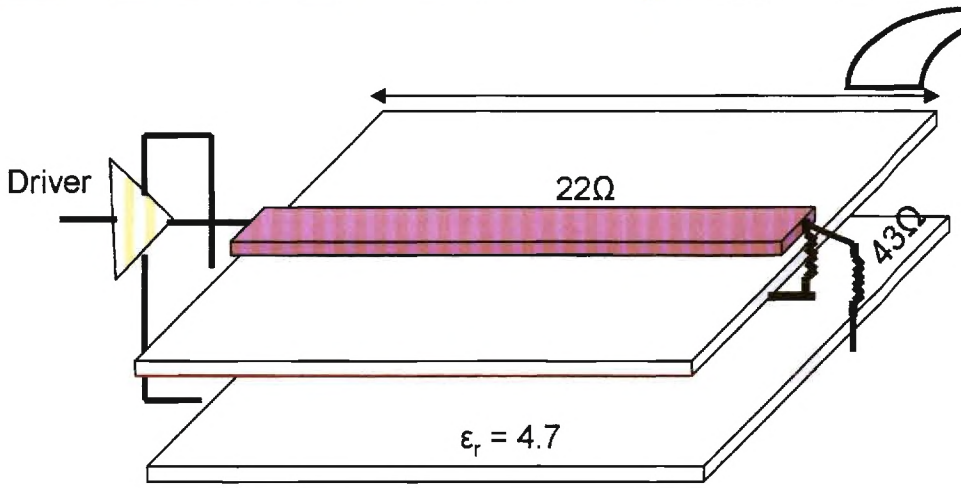

Propagation delay is appreciable in long lines

Affects timing and eye patterns

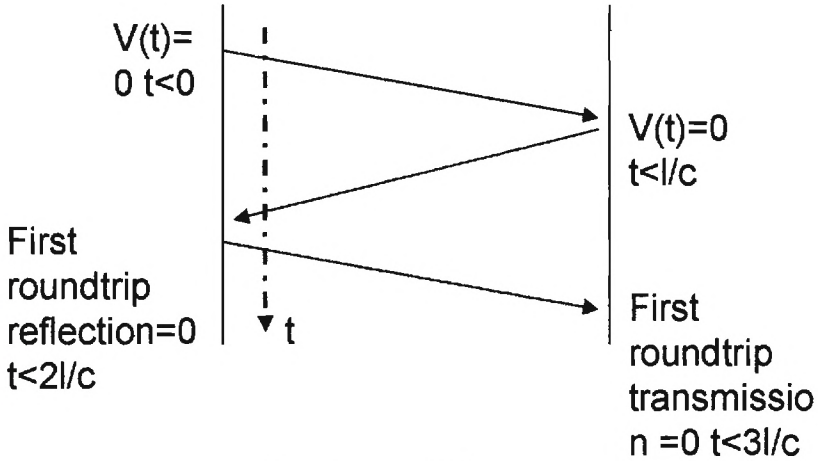

Bounce Diagram

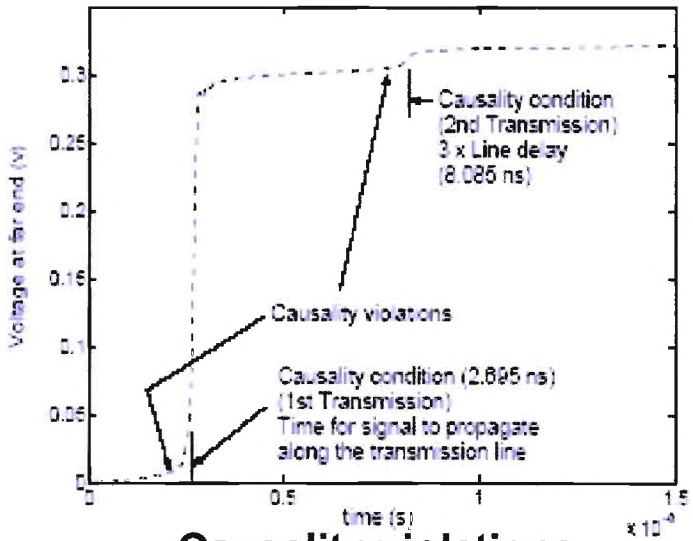

Causality violations

Need for Scalability and Including Arbitrary SPICE Circuits

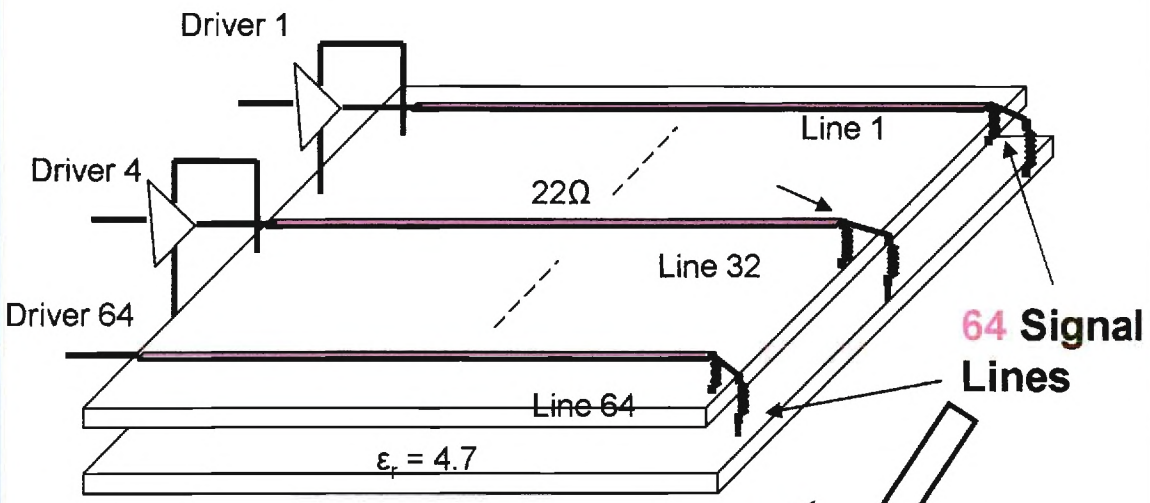

128 port PDN
250 port system network
130 ports after port reduction
(Large problem sizes are often encountered)

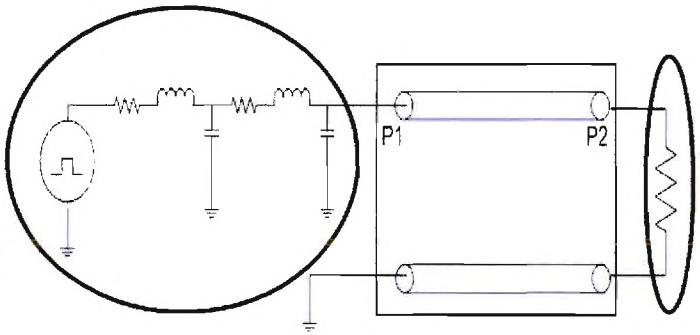

Terminations can be arbitrary SPICE circuit

Prior Work

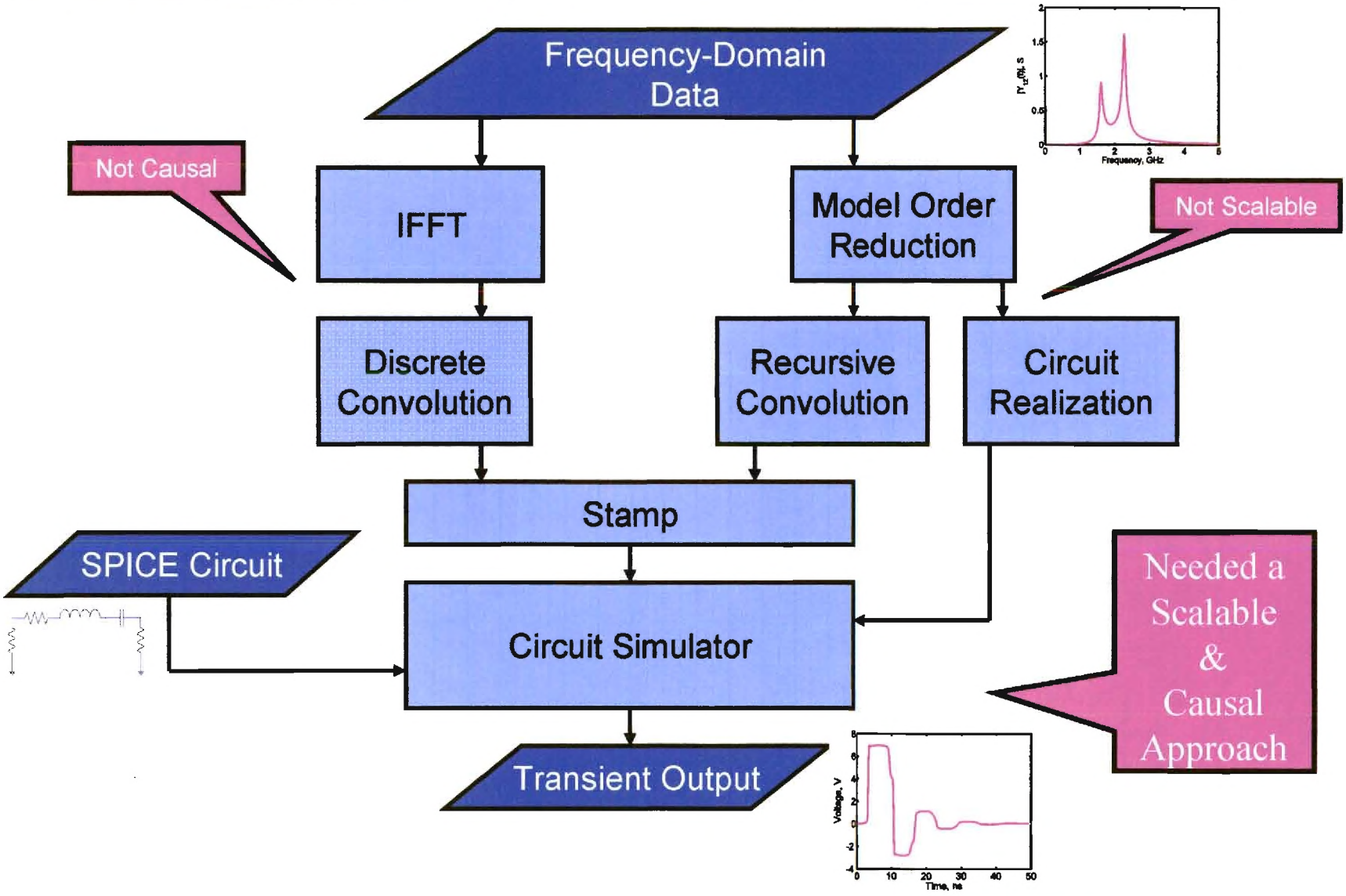
Frequency-Domain Data
Not Causal
IFFT
Model Order Reduction
Not Scalable
Discrete Convolution
Recursive Convolution
Circuit Realization
Stamp
SPICE Circuit
Circuit Simulator
Needed a Scalable & Causal Approach
Transient Output
Frequency, GHz
Voltage, V
Time, ns

Prior Work – Scalable + Causal Approach

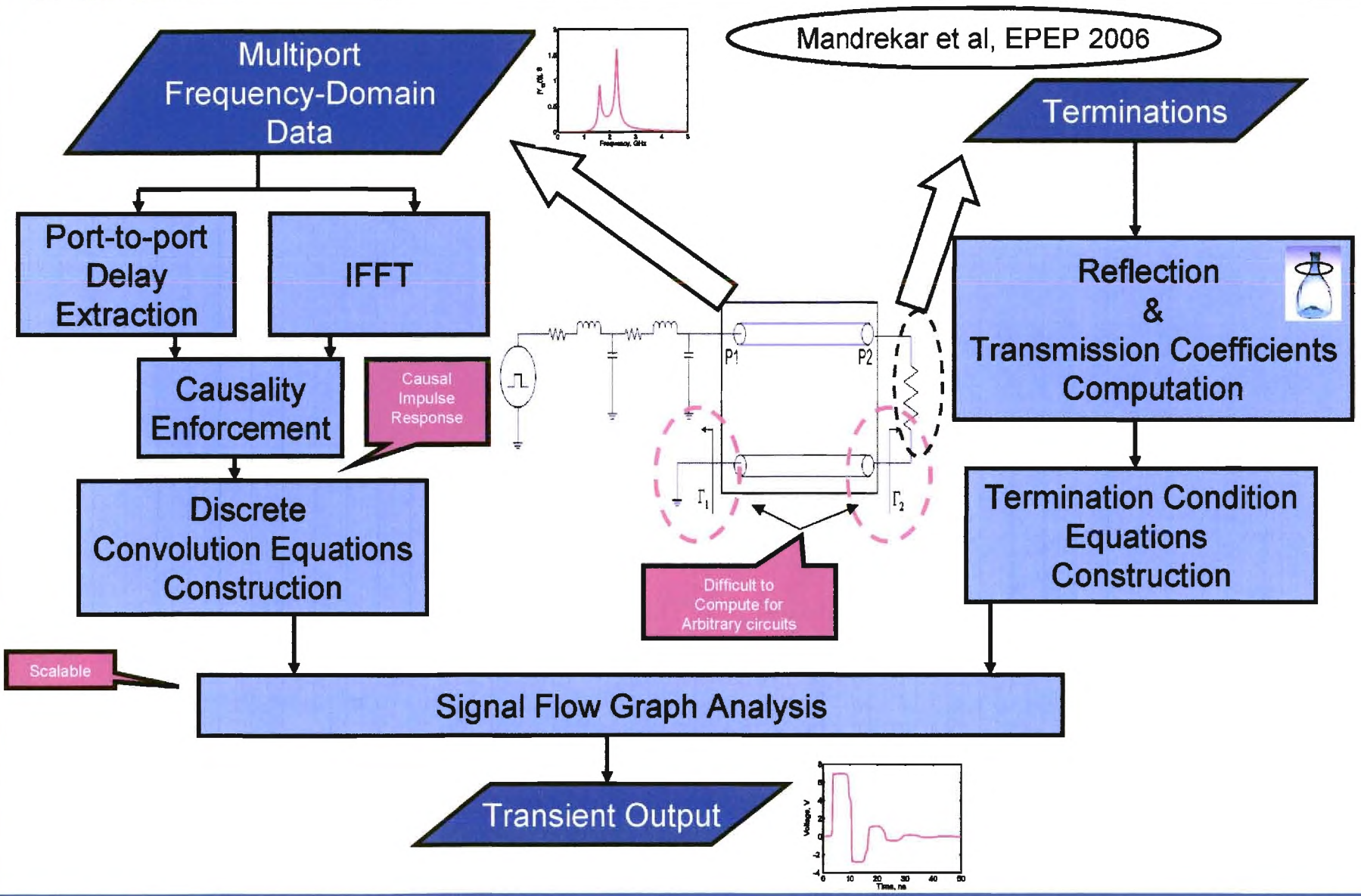

Present Work – Scalable + Causal + Arbitrary SPICE Circuits Approach

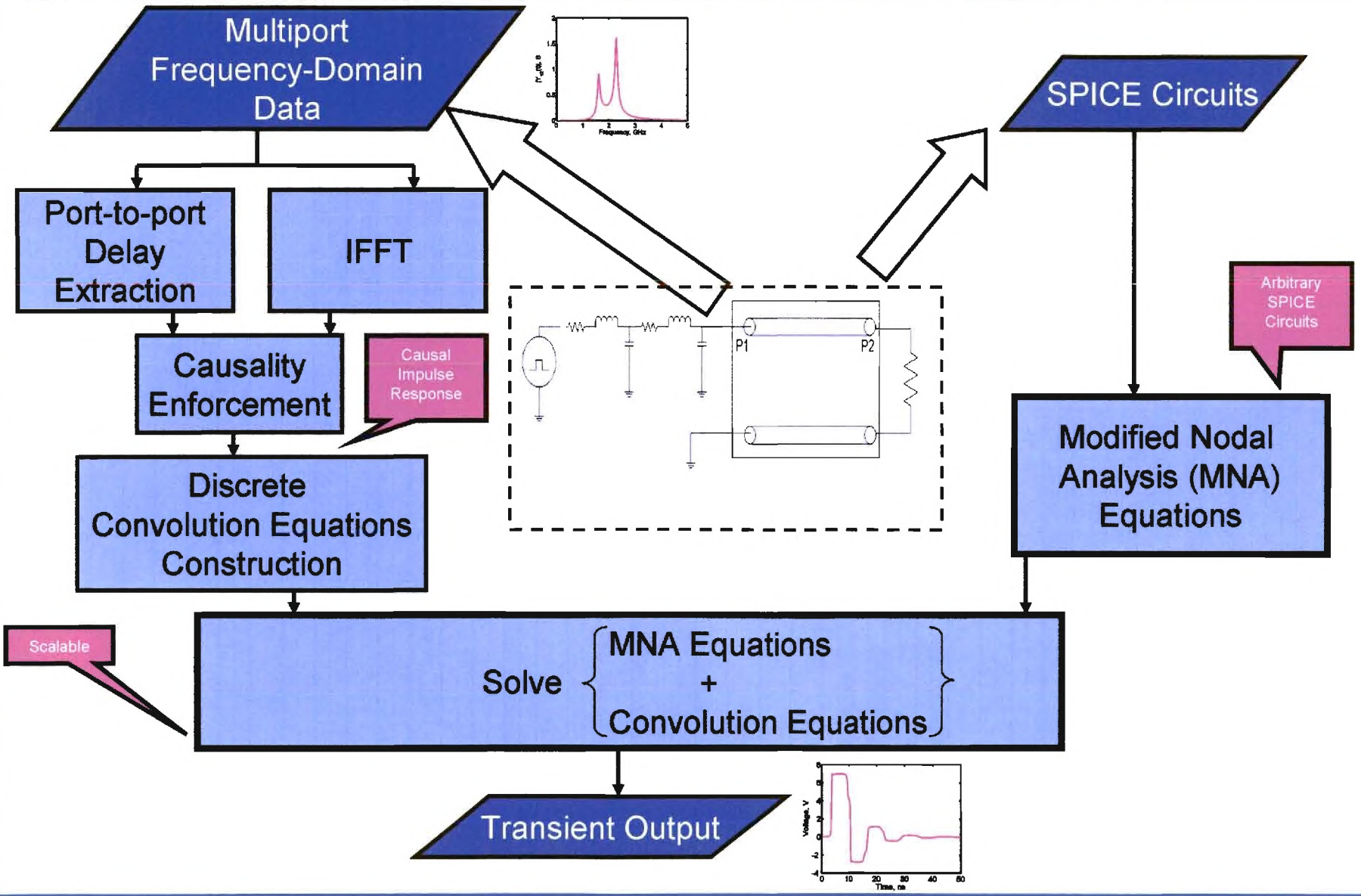

Results – Example 1(1)

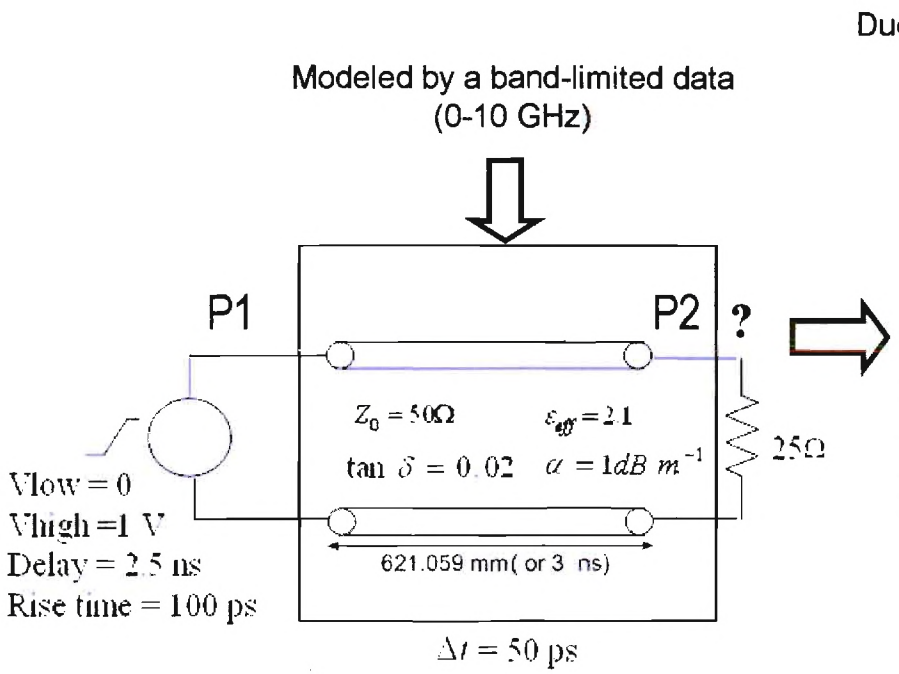

Step Response of a transmission line

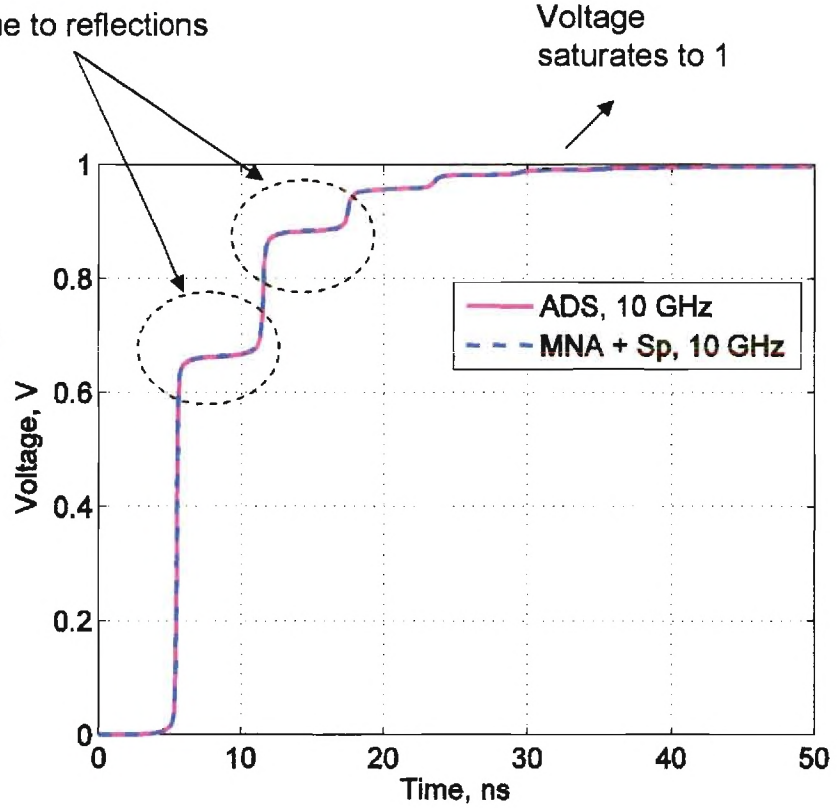

Voltage at P2

MNA-SP
is Accurate

For comparison with ADS, causality has not been enforced in MNA_SP

Results – Example 1(2)

Effect of enforcing causality

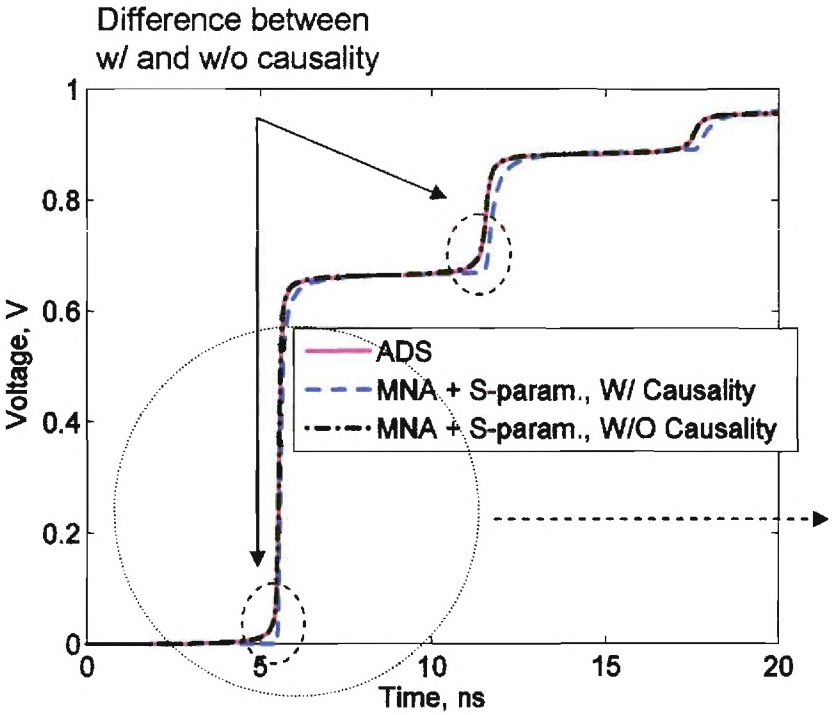

a) Voltage at P2

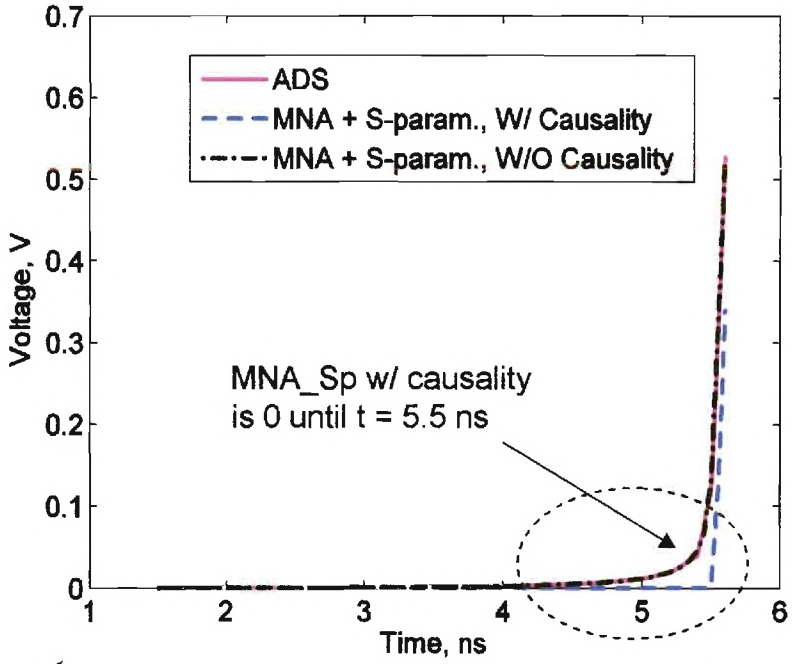

b) Voltage at P2 zoomed

MNA-SP models Causality

Results – Example 2

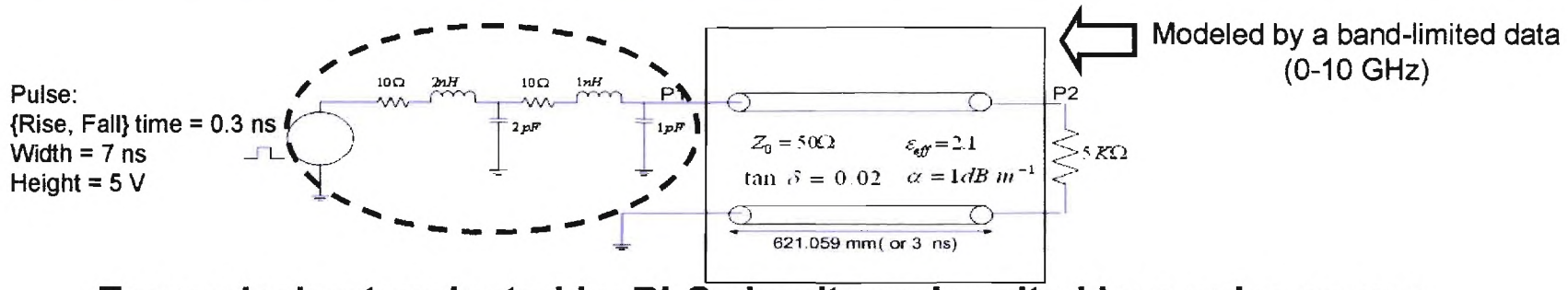

Transmission terminated by RLC circuits and excited by a pulse source

(Termination values borrowed from *)

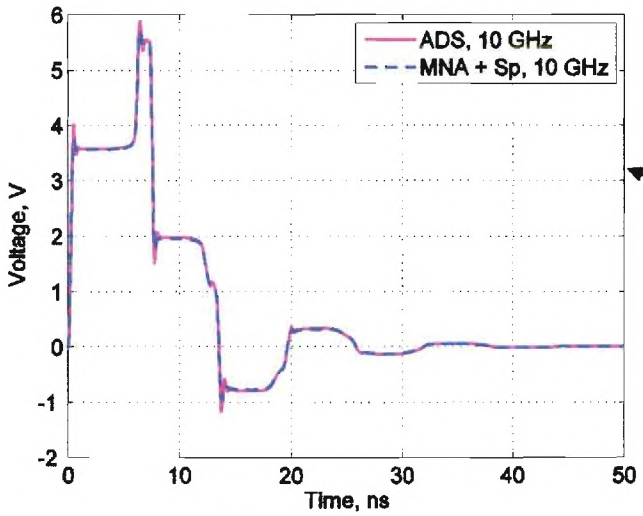

a) Voltage at P1

MNA-SP takes Arbitrary SPICE Circuit

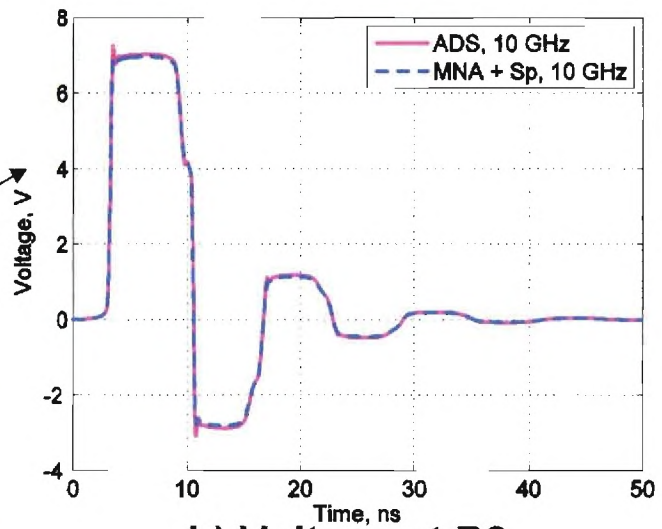

b) Voltage at P2

* W. T. Beyene et al, "Efficient transient simulation of high-speed interconnects characterized by sampled data," *IEEE Trans. on Components, Packaging, and Manufacturing Technology – Part B*, Vol. 21, No. 1, Feb. 1998.

Results – Example 3

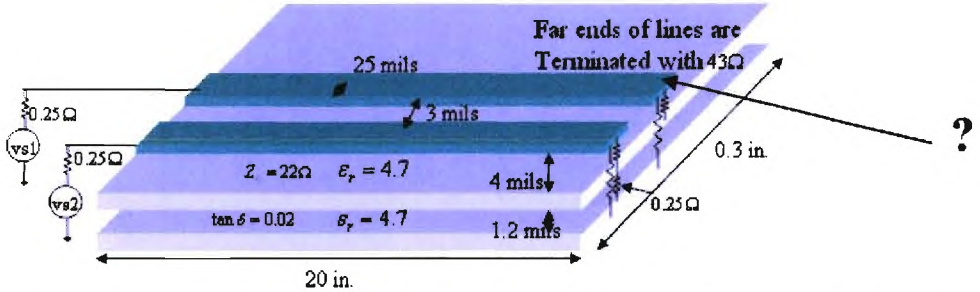

Two transmission lines referenced to nonideal power-ground plane pair

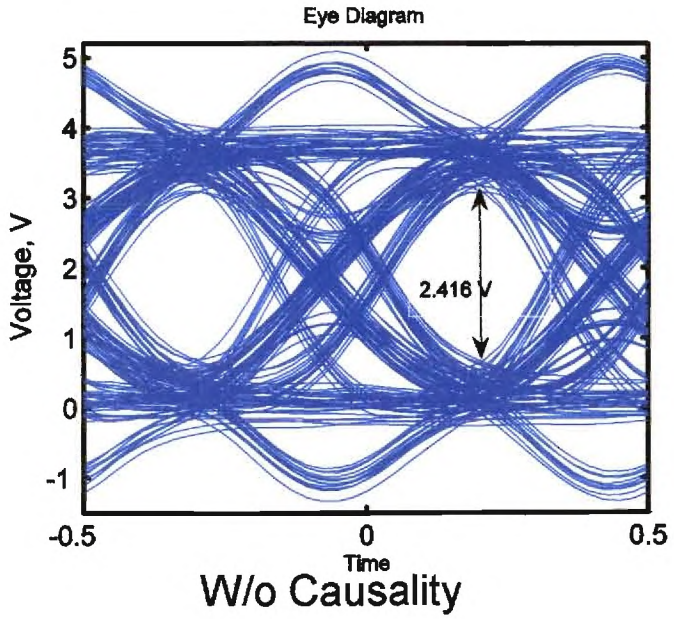

140 mV difference in eye opening

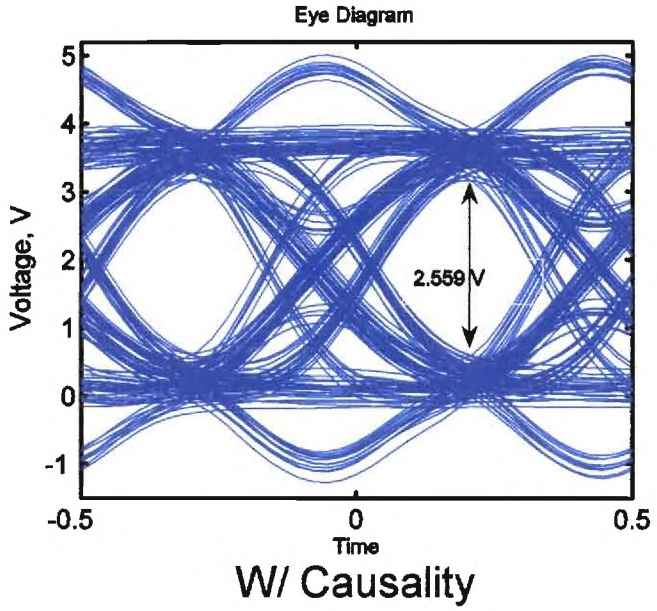

Results – Example 4

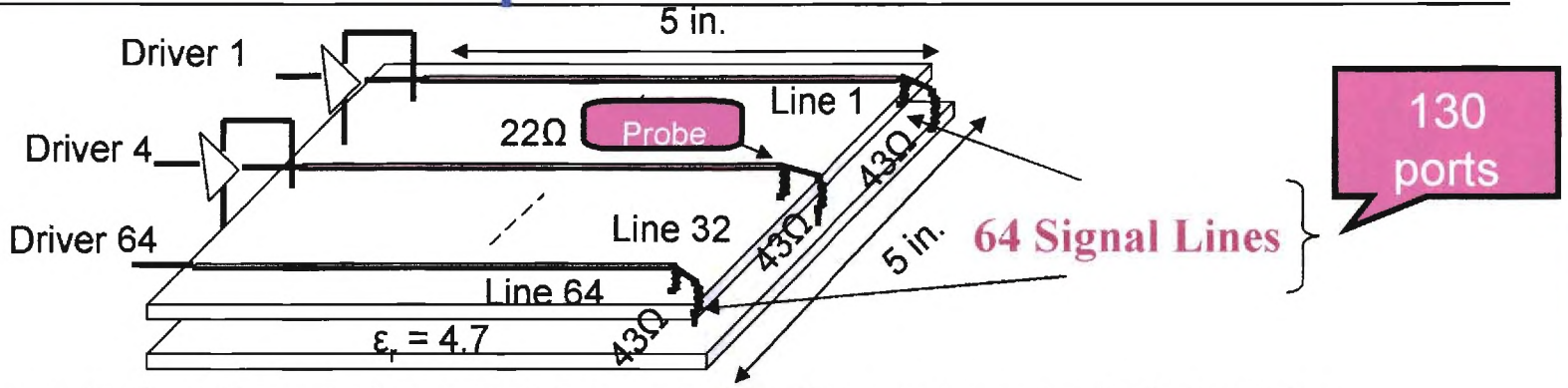

64 transmission lines referenced to a nonideal power-ground plane pair

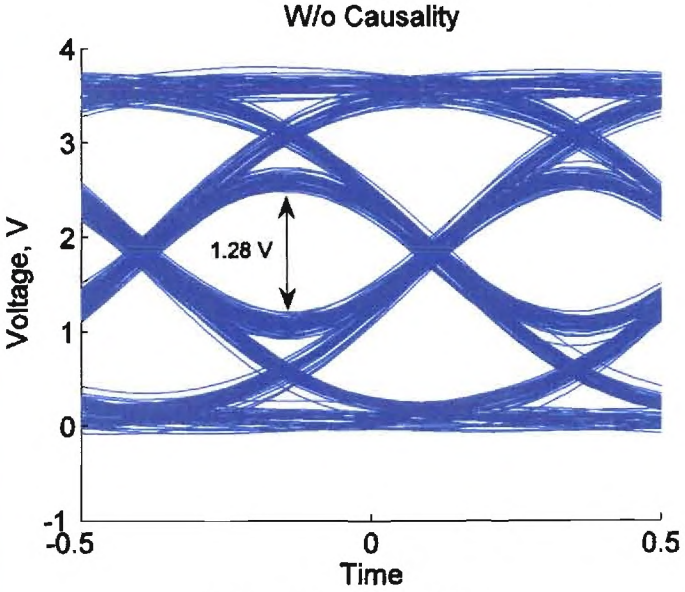

W/o Causality

20 mV difference in eye opening

MNA-SP is Scalable

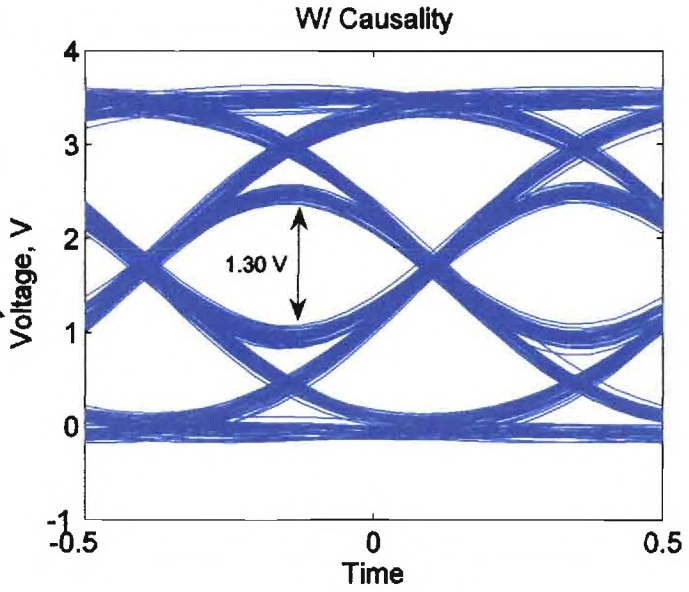

W/ Causality

Summary & Future Work

- Summary:
  - Transient Simulation with S-parameters:
    - Causal
    - Scalable
    - Includes arbitrary SPICE circuits.
- Future Work:
  - Robustness of Simulation for Frequency-Data from Different Types of Systems